

SOLAR ROTATIONAL RADIAL GRADIENT INVERSION USING RING DIAGRAM ANALYSIS OF 10 YEARS OF GONG DATA

A. Zaatri¹, F. Hill², I. Gonzalez-Hernandez², R. Komm², T. Corbard³

¹Centre de recherche en astronomie, astrophysique et géophysique, BP64, Bouzaréah, Algiers, Algeria

²National Solar Observatory, 950 N. Cherry Avenue, Tucson, AZ

³Laboratoire Lagrange, Université Nice Sophia-Antipolis, Observatoire de la Côte d'Azur, Bd. de l'Observatoire, 06304 Nice, France

ABSTRACT

We report on first results of the inversion of the radial gradient of sub-photospheric angular velocity using Ring diagram analysis. The angular radial gradient profiles as obtained from our inversion are smoother than those estimated using numerical radial derivatives of the zonal flows. The inversion has been performed for 10 years of GONG data (years: 2002 – 2011; Carrington Rotations: 1985 - 2118). We find that this radial gradient is mostly negative from near surface layers to about 16 Mm below the photosphere and for $[-52.5; 52.5]$ latitude range. Nonetheless, a positive gradient is found at high northern latitudes before and after the extended solar minimum between cycles 23 and 24.

INVERSION OF THE RADIAL GRADIENT OF ANGULAR VELOCITY

In order to measure the solar rotational radial gradient, we need a formula that links it to an observable quantity, so that it can be inverted using observational data. Hence, we first consider the relation between a frequency perturbation of a solar acoustic mode (i) in X direction (rotational axis) U_x^i and the velocity flow along the same axis V_x , assuming the plane wave approximation:

$$U_x^i = \beta^i \int_0^R K^i(r) V_x(r) dr \quad (1)$$

$K^i(r)$ is the rotational kernel of the proper acoustic mode i
 β^i is a normalization parameter, added to make the kernels unimodular i.e. $\int_0^R K^i(r) dr = 1$

Moreover, the integral in the right hand side of equation (1) can be integrated by part such as:

$$\int_0^R K^i(r) V_x(r) dr = \tilde{K}^i(R) V_x(R) - \int_0^R \tilde{K}^i(r) \frac{V_x(r)}{dr} dr, \quad \tilde{K}^i(r) = \int_0^r K^i(r') dr' \quad (2)$$

Finally, the following equation is obtained from equations (1) and (2):

$$(U_x^i + V_{track}) + \tilde{\beta}^i \tilde{k}^i(R) [V_x(R) + V_{track}] = \tilde{\beta}^i \int_0^R \tilde{k}^i(r) \frac{V_x(r)}{dr} dr, \quad (I)$$

Surface angular velocity

$$\begin{cases} \tilde{\beta}^i = \beta^i \int_0^R \tilde{K}^i(r) dr \\ \tilde{k}^i(r) = -\frac{\tilde{K}^i(r)}{\int_0^R \tilde{K}^i(r) dr} \end{cases}$$

Equation (I) can be inverted to get the angular radial gradient $\frac{V_x(r)}{dr}$, knowing the frequency shifts U_x^i and the surface terms in the right hand side.

NB: V_{track} is the tracking rate. It is written explicitly because the region of interest is tracked before measuring the frequency shifts in x direction using ring diagram analysis.

MEASURING THE GRADIENT USING RING DIAGRAM ANALYSIS

We use the Regularized Least Squares inversion method (RLS) to invert equation (I). We use the frequency shifts as obtained using ring diagram analysis of 1664 tracked tiles extracted from GONG dopplergrams (1min cadence) with an angular extension of $15^\circ \times 15^\circ$ centered at disk center. We use Snodgrass (1984) tracking rate and integrate the rotational kernels obtained from model S (Christensen-Dalsgaard et al. 1996) in order to get the $tilt$ kernels given in equation (2). The resulting resolution kernels are shown in figure 1 for different values of the regularization parameter λ and for two target depths (5Mm and 8Mm). Very low λ values cause the appearance of bumps close to the surface and very high λ values spread the kernels out. Thence, we choose $\lambda=5$ for our inversion.

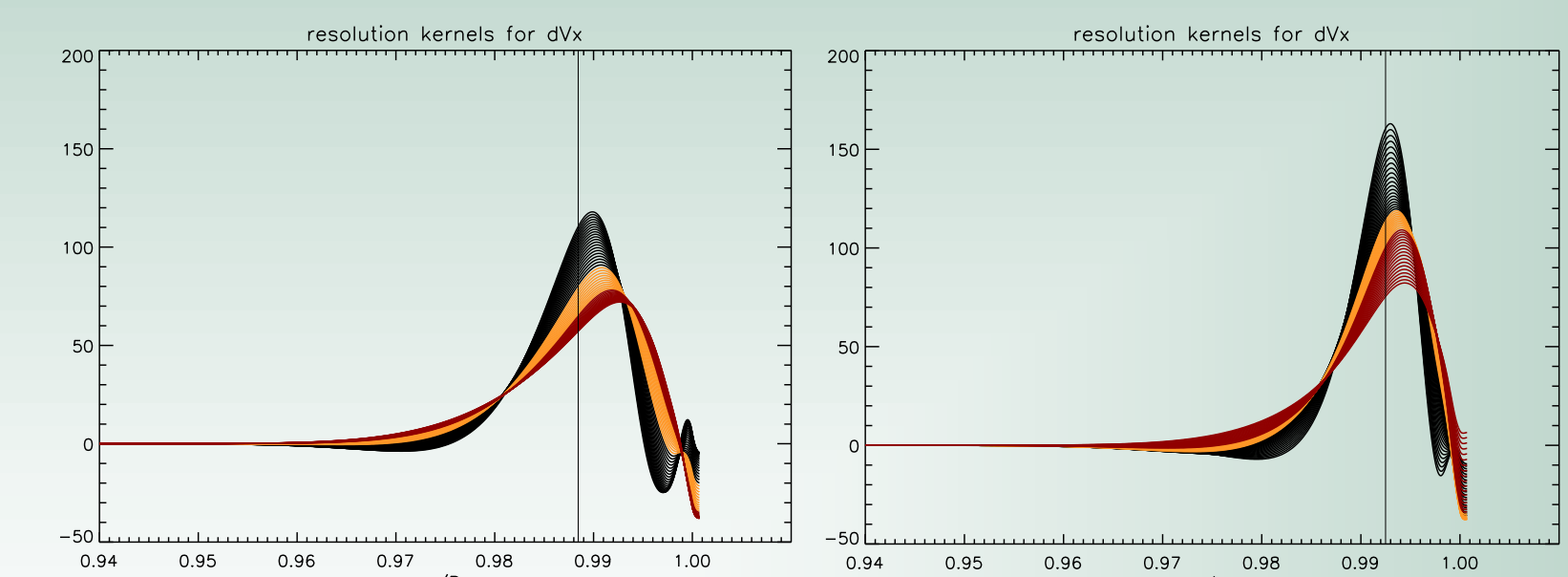


FIGURE 1. resolution kernels for a given depth target (also given by the vertical lines); lower panel: 5Mm, upper panel: 8Mm and a set of regularization parameter values λ ; black: $0.1 < \lambda < 1.26$, orange: $1.5 < \lambda < 5$, red: $6 < \lambda < 50$.

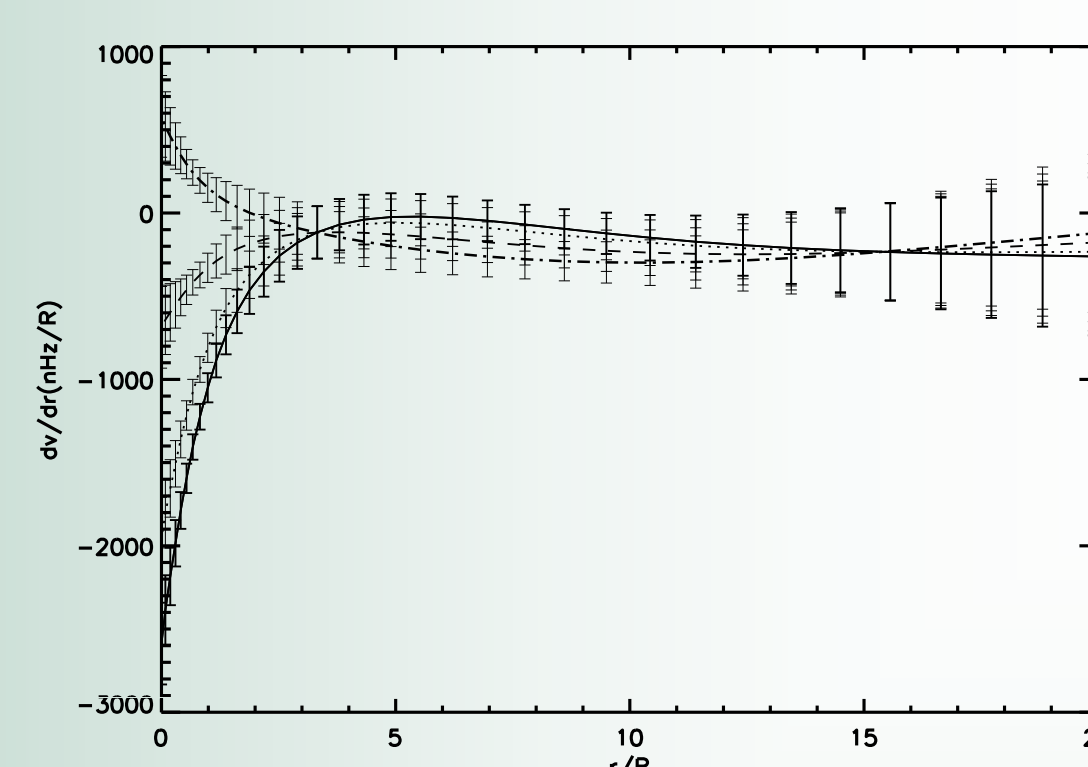


FIGURE 2. Rotational Radial Gradient for different surface velocity values of a patch located at disk center. Full: 5m/s, dotted: 10m/s, dashed: 20m/s, dash-dotted: 30 m/s

Surface angular velocity is needed to perform this inversion (equation (I)). In order to study its effect on the measurement of the angular radial gradient, we have taken several values of the surface velocity and applied the inversion for a patch located at disk center (figure 2). We found that the surface velocity is only relevant at the very first 3Mm below the surface. For now, we will not consider rigorously this quantity in our inversion and will take $V_x(R) = 0$ at all latitudes. Consequently, we trust our results from 3Mm below the surface and deeper.

For the long term study of the radial gradient of angular velocity at different latitudes of the solar disk and a range of depths, we use long time series of Global Oscillation Network Group (GONG) dopplergrams to which we apply the ring-diagram analysis (Corbard et al. 2003) using the dense pack technique (Haber et al. 2002). Each dopplergram is divided into a set of 189 overlapping tiles with centers separated by 7.5° in latitude and longitude and covering a range of $\pm 52.5^\circ$ in longitude and $\pm 52.5^\circ$ in latitude. Each tile is tracked during 1664min at the surface rotation and the resulting dense-pack patch is Fourier transformed to get the high degree modes 3D power spectrum. The power spectrum is then fitted with a Lorentzian profile model which incorporates a perturbation term due to the horizontal velocity components. We use the x component of the horizontal velocity from the set of fitting parameters to perform our inversion (this set of parameters is available at <http://gong2.nso.edu/archive/patch.pl?menutype=h>). In this way, (daily) latitude-longitude maps of the rotational radial gradient are created for a set of depths down to 16Mm.

ROTATIONAL RADIAL GRADIENT FOR 10 YEARS OF GONG DATA

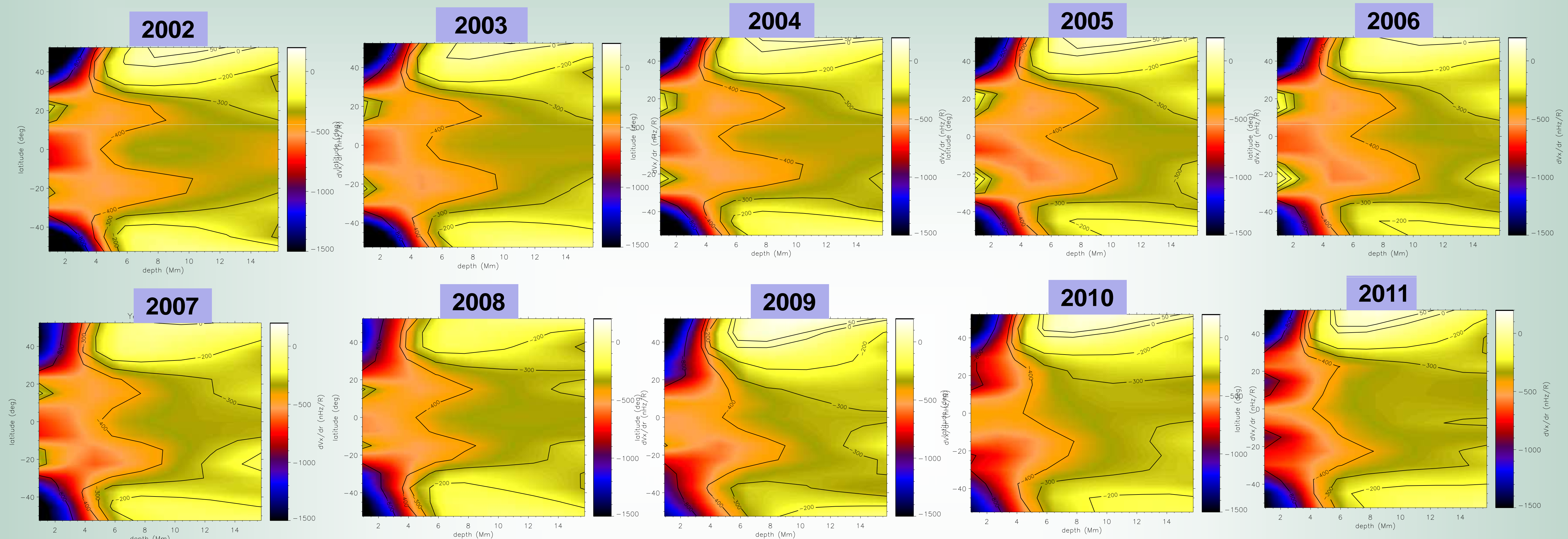


FIGURE 3: Sub-surface radial gradient of angular velocity averaged over each mentioned year for the latitude range $[-52.5, 52.5]$ and depths down to 16Mm.

We apply our inversion to 10 years of Global Oscillation Network Group (GONG) data (2002 - 2011). After generating the daily maps of the rotational radial gradient, we average them over the longitude range for each latitude and depth. The daily gradients are then averaged over one Carrington rotation and finally averaged over roughly one year. The resulting maps are shown in figure 3 from year 2002 to year 2011. Even though, the first 3Mm are included in the maps, we will ignore them because of the poor consideration of the surface velocity in our inversion. These maps highlight the following features:

- the gradient is mostly negative at all depths and latitudes, except for high northern latitudes for the years before 2007 and after 2008.
- all the maps show asymmetric bumps of the gradient at mid latitudes where its amplitude is higher than its equatorial amplitude for the same depth. This is in contradiction with previous measurements using f-modes analysis of MDI data for the first half of cycle 23, where the rotational radial gradient was found to be constant (-400 nHz/R) at latitudes between 0 and 30° (Corbard and Thompson 2002).
- The extension of these bumps in depth is deeper during the last years of cycle 23 (ie. 2002, 2003, 2004, 2005, 2006) than during the first years of cycle 24 (2010, 2011)
- Except for these bumps, the radial gradient amplitude decreases with latitude at a given depth and tends to become positive at higher latitudes.

Our preliminary results on the measurement of the rotational radial gradient show that it has a more complicated behavior than what previous studies have found. In the near future, we will look more carefully on the surface velocity in order to improve our measurements in the first 3Mm. We will also do further analysis on the relation between magnetic activity and the long term behavior of the rotational gradient.

REFERENCES

1. Snodgrass, H.B.: 1984, *Solar Phys.* 94,13.
2. Christensen-Dalsgaard, J., Däppen et al.: 1996. *Science*, 272, 1286 – 1292.
3. Haber, D.A., Hindman, B.W., Toomre, J., Bogart, R.S., Larsen, R.M., and Hill, F.: 2002, *Astrophys. J.* 570, 885.
4. Corbard, T., Toner, C., Hill, F., Hanna, K.D., Haber, D.A., Hindman, B.W., and Bogart, R.S.: 2003, in H. Sawaya-Lacoste (ed.), *Local and Global Helioseismology: The Present and Future*, (ESA SP-517), ESA, Noordwijk, Netherlands, p. 255.
5. Corbard, T., Thompson, M. J.: 2002, *solar physics*, 205, 211